Engineering with Computers (2020) 36:455–474
https://doi.org/10.1007/s00366-019-00708-1

ORIGINAL ARTICLE

Application of a Bayesian hierarchical model to system identification of structural parameters

Shinyoung Kwag[1] · **Bu Seog Ju**[2]

Received: 27 February 2018 / Accepted: 14 January 2019 / Published online: 4 February 2019

Abstract
System identification (SI) is a key step in the process of evaluating the status or condition of physical structures and of devising a scheme to sustain their structural integrity. SI is typically carried out by updating the current structural parameters used in a computational model based on the measured responses of the structure. In the deterministic approach, SI has been conducted by minimizing the error between calculated responses (using the computational model) and measured responses. However, this brought about unexpected numerical issues such as the ill-posedness of the inverse problem, which likely results in non-uniqueness of the solutions or non-stability of the optimization operation. To address this issue, Bayesian updating enhanced with an advanced modeling technique such as a Bayesian network (BN) was introduced. However, it remained challenging to construct the quantitative relations between structural parameters and responses (which are placed in conditional probability tables: CPTs) in a BN setting. Therefore, this paper presented a novel approach for conducting the SI of structural parameters using a Bayesian hierarchical model (BHM) technique. Specifically, the BHM was integrated into the Bayesian updating framework instead of utilizing a BN. The primary advantage of the proposed approach is that it enables use of the existing relations between structural parameters and responses. This can save the computational effort needed to construct CPTs to relate the parameter and response nodes. The proposed approach was applied to two experimental structures and a realistic soil-slope structure. The results showed that the proposed SI approach provided good agreement with actual measurements and also gave relatively robust estimation results compared to the traditional approach of maximum likelihood estimation. Hence, the proposed approach is expected to be utilized to address SI problems for complex structural systems and its computational model when integrated with a statistical regression approach or with various machine learning algorithms.

Keywords Bayesian updating · Bayesian hierarchical model · System identification · Measurement · MCMC sampling

1 Introduction

The structure health monitoring has been recently utilized in diverse structural systems [1, 2] for several objectives. This is mainly to measure structural characteristics under various loading conditions using instruments, to assess the condition or "health" of a physical structure, and to maintain and manage its integrity based on these measurements and assessments. Because advances in instrumentation and data processing technologies are rapidly being made, the amount of valuable data that can be accumulated has increased, and their accuracy of such data has been much improved. Such information with the increased accuracy can now effectively be used to identify actual structure system parameters. This is called as a process called system identification (SI), which is a key step in evaluation of the condition of a structure (its health) and in devising a scheme to sustain its structural integrity. Also, the utilization of the information in the SI process plays a key role in reducing uncertainties in structural model parameters. Under such basic background, the focus of this study lies in dealing with the system identification (SI) problems of various structural systems. From this perspective, we described the literature review and the state-of-the-art studies on this topic with respect to the structural engineering field.

Currently, SI is usually conducted in a deterministic or probabilistic manner. However, the deterministic approach

✉ Bu Seog Ju
bju2@khu.ac.kr

[1] Korea Atomic Energy Research Institute, Daejeon, South Korea

[2] Department of Civil Engineering, KyungHee University, Yongin-si, Gyeonggi-do, South Korea

has fundamental numerical issues such as non-stability and non-uniqueness of solutions, which may not easily be overcome. The probabilistic method using Bayesian strategies in the SI problem requires refined modeling techniques to deal with the relationships between components, subsystems, and the main system. In this context, though Bayesian network (BN) was recently introduced in the SI problem, the existing BN-based techniques require considerable efforts to identify such relationships.

To be more specific, in a deterministic approach, the SI is handled by minimizing the discrepancies between calculated responses (using a theoretical or numerical model) and measured responses [3] and thus can be formulated as an optimization problem. For this reason, deterministic SI techniques frequently fall into local solutions or suffer nonstability of the solution (i.e., ill-posedness) [4–6]. Moreover, these techniques have a limitation which do not easily deal with uncertainties in structural parameters or measured data in a single consistent framework.

In a probabilistic approach for the SI, the parameters of the structure system are treated as probability density functions to account for uncertainties in the parameters [7]. Therefore, the measured data obtained from the sensors need to be incorporated into the current probabilistic models of structural parameters, which can be realized via the application of a Bayesian updating framework to SI. Bayesian updating enables accommodation of new observations into the current prior probabilistic models by updating the parameters of the prior probabilistic models. Since the Bayesian updating concept was introduced in the 1960s, it has been applied to many engineering fields. Benjamin and Cornell [8] first illustrated how to use Bayesian updating to enhance engineering decision-making processes by employing examples of material testing and geotechnical site investigations. Ang and Tang [9] summarized application of the Bayesian approach to real-life problems using structure, transportation, and hydrology engineering examples. Specifically, for the SI applications, the Bayesian approach has been used for identifying structural systems under dynamic loading [10–12] and for model calibration with data for rainfall or discharge measurements [13]. However, because the SI problem becomes more complicated when applied to systems involving inter-correlated parameters in multiple layers, it is necessary to use an integrated modeling technique that makes full use of the merits of Bayesian updating. This is one of the primary reasons why the concept of BN was utilized in the SI problem.

A BN is a graphical representation of a set of conditional independence assumptions; thus, it accordingly constitutes a compact joint probability distribution between random variables. Due to this characteristic, the BN allows efficient probabilistic inference within the Bayesian updating framework when given new observations (also called evidence). The BN basically utilizes nodes denoting random variables, arrows showing relationship between linked nodes, and conditional probability tables (CPTs) indicating how linked nodes are quantitatively related. The BN has been widely used in the fields of computer science, social sciences, business, public affairs, and engineering. Specifically, the examples of BN application for structural engineering were mainly concentrated on improvements in structural reliability evaluations [14] and risk assessments [15–21].

There were several examples that used the BN concept for the purpose of the SI. These were the studies on the robust updating of nonlinear structural models [22], prediction for remaining bridge strength [23], and probabilistic identification of the spatial distribution of structural parameters [24]. The main feature of these BN-based SI approaches is the presence of discrete nodes given by discretized intervals, where the corresponding conditional probabilities given for each interval (i.e., CPTs) need to be computed via Monte Carlo Simulation (MCS) methods. In each MCS, a combination of selected intervals is employed to calculate the responses from the defined numerical model. Hence, the computations for constructing CPTs have demanded a large cost. Richard et al. [22] also pointed out that one major drawback when using a BN for the SI is the computational time required for estimating the CPTs.

However, we do not need to evaluate the CPTs if the nodes are considered as continuous and the relationships among the nodes are given in closed-functional form. This situation is possible when the relationships between the desired responses and structural system parameters can be obtained from an explicitly known mechanics model or from a surrogate model regressed from a large amount of data. If we know the node relationship from such models, we can intuitively solve the SI problem by leaving the parameters to follow the continuous distribution as they are. And this leads to completely removing the computational cost by not constructing CPTs but utilizing existing relations. The process of replacing CPTs with closed functional forms by treating the nodes as continuous in multiple layers is exactly the one that the Bayesian hierarchical modeling (BHM) does. In Bayesian statistics, the BHM is a general concept in estimating the parameters of posterior distributions. Thus, the correctness of the BHM has already been proved, theoretically [25]. This technique is powerful when data/information are available on several different levels of observational units. Due to such features, the BHM has been recently applied to diverse engineering fields. Yet, the BHM concept is a still quite new in the structural engineering area.

Therefore, in this paper, a novel approach for SI of structural parameters that combines the Bayesian updating strategy with the BHM technique is proposed. This proposed BHM-based SI approach enables use of the existing relations between structural parameters and responses. This can avoid

the additional computational cost of constructing CPTs to relate parameter and response nodes. The approach also allows the analyst to visually understand the interdependencies between random variables and to identify the critical node if necessary. The proposed approach is herein applied to two experimental structures and to a realistic soil-slope structure as SI examples. The effectiveness of the approach is verified by comparative studies with the existing statistical approach and actual measurements. Moreover, if the proposed approach is combined with a statistical regression approach or various machine learning algorithms, such a combination is expected to effectively handle the SI even for complex structural systems and its computational model.

This paper is organized as follows. In Sect. 2, the basic concepts of Bayesian updating and BHM are presented. The Bayesian updating method includes a computational scheme to solve the formulated Bayesian theorem. In Sect. 3, we describe the proposed approach adopting Bayesian updating and BHM for SI of structural parameters. Section 4 illustrates the effectiveness of the proposed SI approach by application to two experimental structures and a soil-slope structure. To do this, we basically compare the actual measurements of the experiments with the results of the proposed method. Section 5 concludes with a summary and discussion.

2 Basic concepts

Before presenting the BHM-based SI method, which is the core of this research, let us look at the key concepts for understanding the method. This method is mainly based on two major concepts, a Bayesian updating concept and the BHM technique. In the next subsections, we will discuss these concepts.

2.1 Bayesian updating

Bayesian updating is an inference technique in which Bayesian theorem is employed to update the current degree of belief based on newly observed data. This concept has been widely used in diverse engineering fields that need to deal with problems of an uncertain nature. Mathematically, this can be expressed in the following equation [26]:

$$p(\boldsymbol{\theta}|\mathbf{y}) = \frac{p(\mathbf{y}|\boldsymbol{\theta})p(\boldsymbol{\theta})}{p(\mathbf{y})} = \frac{p(\mathbf{y}|\boldsymbol{\theta})p(\boldsymbol{\theta})}{\int p(\mathbf{y}|\boldsymbol{\theta})p(\boldsymbol{\theta})d\boldsymbol{\theta}} \propto p(\mathbf{y}|\boldsymbol{\theta})p(\boldsymbol{\theta}) \quad (1)$$

where $p(\boldsymbol{\theta})$ is a prior probability distribution; $p(\mathbf{y}|\boldsymbol{\theta})$ is a likelihood function that is also expressed as $L(\mathbf{y}|\boldsymbol{\theta})$; and $p(\boldsymbol{\theta}|\mathbf{y})$ is a posterior probability distribution. Note that traditional statistics uses the maximum likelihood estimation (MLE) approach in which it seeks a point value for $\boldsymbol{\theta}$ that maximizes the likelihood. Such an MLE approach does not consider prior distributions, unlike the Bayesian approach. Specifically, as shown in Eq. [1], to obtain the posterior distribution, we need to integrate the denominator $p(\mathbf{y}|\boldsymbol{\theta})\bullet p(\boldsymbol{\theta})$. However, if a total number of parameter (θ) is increased from a single to several, multiple integrals would be required, and, accordingly, the integration would become mathematically intractable. Hence, an approximating algorithm is necessary to cope with such a problem. Usually, an MCMC (Markov Chain Monte Carlo) sampling method [e.g., Metropolis–Hastings (MH) sampling, Gibbs sampling, Slice sampling, rejection sampling, or importance sampling] has been utilized for the purpose of conducting such integral calculus. This sampling method directly extracts samples from the targeted distribution $p(\mathbf{y}|\boldsymbol{\theta})\bullet p(\boldsymbol{\theta})$. The samples obtained from such a process are utilized to estimate the posterior distribution because the targeted distribution is proportional to the posterior distribution [27]. More detailed information on Bayesian updating and its various sampling algorithms can be found in the literature [25]. In this study, both the MH and Gibbs sampling techniques were utilized. The reason for adopting both the techniques was to confirm and show that the SI approach proposed in this study was not restricted to a particular sampling algorithm. In this study, for the brevity of the manuscript, the detailed introduction on both of sampling algorithms is not presented. But, for the purpose of effectively understanding the Bayesian updating concept, the brief description on the MH algorithm is included in the following paragraph.

The MH sampling technique is one of the MCMC sampling methods, which conducts an iterative process [27]. Table 1 specifically describes this algorithm. Specifically, looking through this table, the process starts by generating an arbitrary sample $x^{(0)}$ in the specified range first, estimates a value of the targeted distribution with respect to $x^{(0)}$, and then assigns the value to *p_old*. It subsequently draws a new sample $x^{(1)}$ based on the proposal distribution and current state $x^{(0)}$, evaluates a value of the targeted distribution regarding $x^{(1)}$, and sets this value to *p_new*. Then, *alpha* is determined as the minimum among the value of one and the ratio of *p_new* and *p_old*, which then becomes the criterion for whether or not to accept a new sample by comparison with a randomly generated number in the range 0–1. The aforementioned procedure is iterated until sufficient points have been obtained within the targeted distribution. Due to these features of the algorithm, the first few samples cannot generally represent the target distribution and so should be discarded when estimating the target distribution based on samples obtained with this algorithm. Also, to describe the target distribution accurately, a large number of samples should be generated, and their convergence should be verified.

Table 1 General pseudo code for Metropolis–Hastings algorithm

```
Generate initial guess x^(0)
Set number of samples n; Set coefficient of variation of proposal distribution cov
Iteration loop k = 0, 1, 2, 3, …, n
    Calculate p_old (x^(k))
    x^(k+1) = x^(k) + x^(k) *cov*randn
    Calculate p_new (x^(k+1))
    alpha = min (1, p_new/p_old)
    r = rand
    if r < alpha,
      accept new point
    else
      keep old point
    end
    k = k+1;
return
```

* Here *p_old* and *p_new* are the estimated targeted distributions according to $x^{(k)}$ and $x^{(k+1)}$; *randn* is a random number generator from a standard normal distribution; and *rand* is a random number generator from a uniform distribution in the range 0–1

2.2 Bayesian hierarchical model

Within the Bayesian updating framework, we often encounter the complex problem of inter-correlated parameters. One example of this problem is the case where random variables form diverse hierarchical layers and such layers are connected with each other. To handle this problem, the Bayesian hierarchical model (BHM) can provide an effective tool to build a statistical model constructed in multiple correlated layers, by which it is also possible to evaluate the parameters of the posterior distribution utilizing Bayesian updating [25]. The model mainly consists of the following three hierarchical layers:

- Data layer : $\mathbf{y}|\boldsymbol{\theta},\mathbf{x} \sim p(\mathbf{y}|\boldsymbol{\theta},\mathbf{x})$
- Process layer : $\boldsymbol{\theta}|\mathbf{x} \sim p(\boldsymbol{\theta}|\mathbf{x})$
- Prior layer : $\mathbf{x} \sim p(\mathbf{x})$

where $\mathbf{y}$ is an observation obtained from the experiments, simulations, fields, etc.; $\boldsymbol{\theta}$ is a parameter dependent on the random variable $\mathbf{x}$; and $\mathbf{x}$ is a random variable following the particular prior distribution $p(\mathbf{x})$. Hence, the final posterior distribution obtained from the model can be represented as the following equation:

$$p(\boldsymbol{\theta}, \mathbf{x}|\mathbf{y}) \propto p(\mathbf{y}|\boldsymbol{\theta}, \mathbf{x}) p(\boldsymbol{\theta}|\mathbf{x}) p(\mathbf{x}) \tag{2}$$

The MCMC method introduced in the previous section can also be utilized to establish the desired posterior distribution using Eq. [2]. For a clearer understanding of the BHM concept, let us consider a simple case in which the distribution from which the observations y_i are drawn is characterized by just a few normally distributed parameters with a mean and standard deviation. The model for this simple example can be described by the following mathematical expressions consisting of three hierarchical layers:

- Data layer : $y_i \sim N(\mu, \sigma_y)$; $i = 1,\ldots,n$
- Process layer : $\mu = a + b$
- Prior layer : $b \sim N(0, \sigma_b)$

where $N(\mu, \sigma_y)$ is a normal distribution with mean μ and standard deviation σ_y, and μ is equal to the sum of the parameters a and b. In this case, b follows a normal distribution $N(0, \sigma_b)$. This model can also be graphically represented as shown in Fig. 1. In this figure, a square and a circle respectively denote a constant node (or deterministic node) and variable node (or stochastic node). The dashed lines and solid lines with arrows represent the deterministic and stochastic relationships, respectively, among linked nodes. The corner-rounded square, called a plate for indices, shows the iterative process that needs to be conducted from $i = 1$ to $i = n$. Finally, in this particular example, the posterior distribution with regard to the prior distribution b can be described as Eq. [3], except for the constant nodes in the prior and process layers.

$$p(b|\mathbf{y}) \propto \prod_{i=1}^{n} \left[p\left(y_i|\mu\right)\right] p(\mu|b) p(b) = \prod_{i=1}^{n} \left[p\left(y_i|f(b)\right)\right] p(b) \tag{3}$$

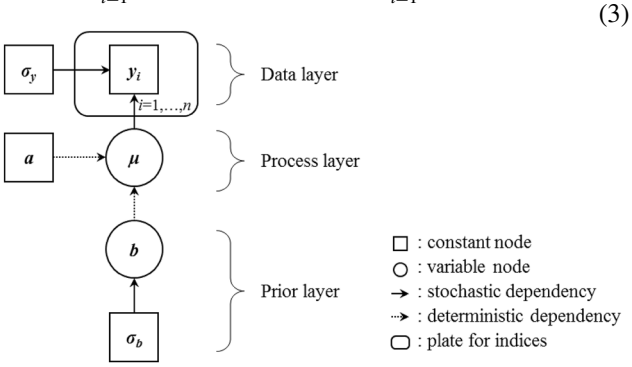

Fig. 1 Simple example of a Bayesian hierarchical model

where $p(-)$ is a defined probability distribution (i.e., normal distribution in the example), and $f(-)$ is a function indicator in the process layer; in this particular example, $f(b) = \mu = a + b$.

In the next section, based on the two key concepts introduced in this section, we will present a BHM-based method for the SI of the structural parameters. In this method, the structural parameters are configured in the prior layer, and the structural responses observed from the measurement are established in the data layer. Finally, the process layer defines the links between the structural parameters and the responses. In the following section, we will specifically explain the proposed approach using a conceptual figure of the overall methodology and a general structural system example.

3 BHM for SI of the structural parameters

The concept of Bayesian updating within the BHM presented above provides the basis for a very powerful environment in which to conduct the SI for structural systems. As discussed earlier, BN-based SI techniques require additional computation costs to construct the probabilistic relationships between the linked nodes of the components, the subsystems, and the main system. Yet, the BHM does not require additional effort when establishing such relationships because it can utilize an explicitly known mechanistic model or a statistical regression structural model. From this perspective, this section describes a general approach for the SI of the structural parameters using the BHM technique. Figure 2 shows a conceptual schematic of the proposed BHM-based SI approach. Specifically looking through this conceptual figure, we first select important parameters of a given structural system. Next, we measure the responses of the structure, such as natural frequencies, displacements, stresses, and strains, under specific loading conditions. We also derive mathematical, physical, or empirical relationships between structural parameters and responses. Based on such information, we establish the BHM model on each layer. Each layer consists of three major layers, called as the prior layer, process layer, and data layer. The prior layer considers the uncertainties of structural parameters already selected and treats them as probability density functions. The data layer defines the measured response as

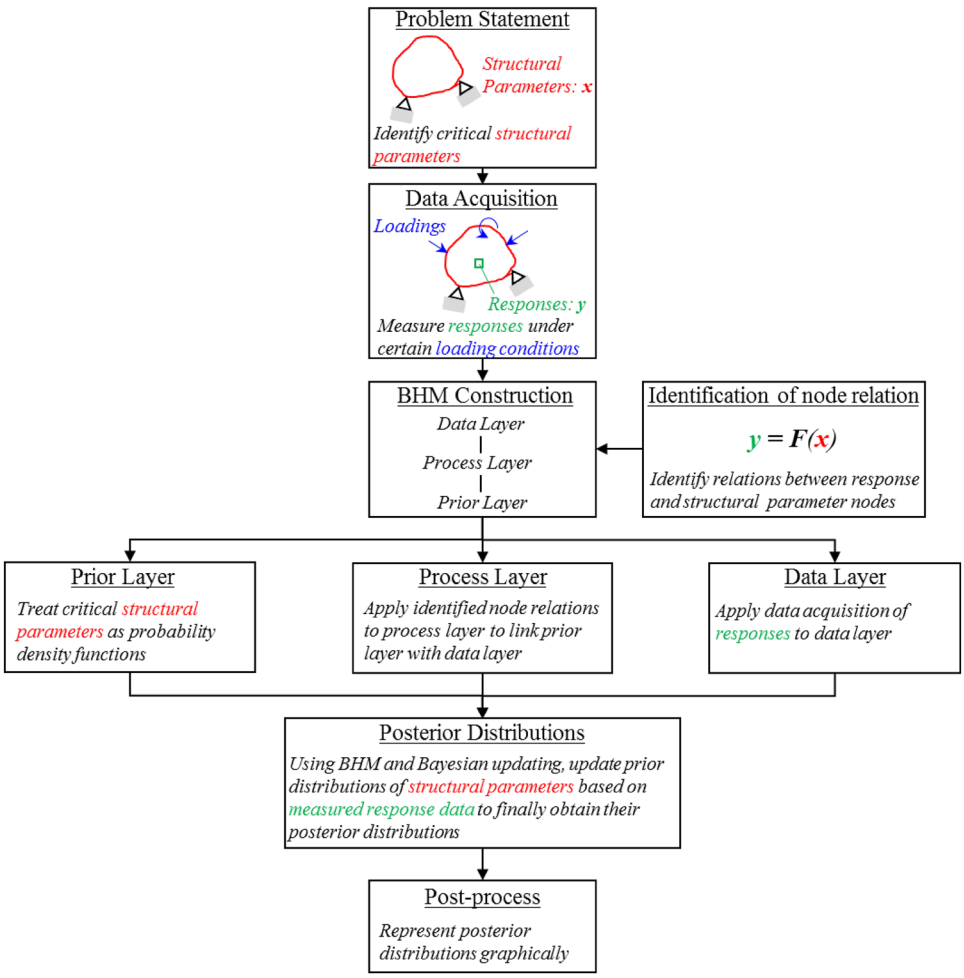

Fig. 2 Conceptual process of the proposed BHM-based SI approach

random variables. The process layer formulates the relationships between probability density functions of the structural parameters of the prior layer and the random variables of the responses of the data layer. This layer is based on mathematical relationships derived between structural parameters and responses. Finally, using the constructed BHM and Bayesian updating concepts, the final posterior distributions of the structural parameters are calculated to reflect the measured response data. The posterior distribution obtained after all these stages is represented as graphical figures or numerical values as a result of a post-processing operation.

To illustrate the key aspect of the proposed method, let us suppose that the BHM is constructed as shown in Fig. 3 through the structural parameters, response measurement, and the relations between structural parameters and responses with respect to a given structural system. The node x_i represents structural parameters and follows a certain distribution *dist* having distribution parameters α_i and β_i due to its uncertainties. Theoretically, the structural response θ_j can be evaluated based on the structural parameters $\mathbf{x} = \{x_1,\ldots, x_l\}$ (i.e., a function of $\mathbf{x}$). Experimentally, the structural response y_{jk} can be independently measured with error σ_{yj}. Thus, the BHM for this structure system can be formulated with the following mathematical expressions:

- Data layer : $y_{jk} \sim N(\theta_j, \sigma_{yj})$; $k = 1,\ldots,n$
- Process layer : $\theta_j = f_j(\mathbf{x})$; $j = 1,\ldots,m$
- Prior layer : $x_i \sim dist(\alpha_i, \beta_i)$; $i = 1,\ldots,l$

If utilizing the Bayesian updating concept based on the defined BHM and the measured data y_{jk}, the prior distributions of the structural parameters reflect the measured data, and these prior distributions accommodating the measurement data are finally updated to the posterior distributions well representing the actual physical state of the structural system. The posterior distributions of x_i thus obtained are proportional to the following equation:

$$
\begin{aligned}
&p\left(x_1,\cdots,x_l|\mathbf{y_{1k}},\cdots,\mathbf{y_{mk}}\right)\\
&\propto \prod_{k=1}^{n}\left[p\left(y_{1k}|\theta_1\right)\cdots p\left(y_{mk}|\theta_m\right)\right]p\left(\theta_1|x_1,x_2,x_3\right)\cdots p\left(\theta_m|x_3,x_4,x_l\right)p\left(x_1\right)\cdots p\left(x_l\right)\\
&= \prod_{k=1}^{n}\left[p\left(y_{1k}|f_1\left(x_1,x_2,x_3\right)\right)\cdots p\left(y_{mk}|f_m\left(x_3,x_4,x_l\right)\right)\right]p\left(x_1\right)\cdots p\left(x_l\right)
\end{aligned}
\tag{4}
$$

As explained in Sect. 2, these posterior distributions are calculated based on Eq. [4] and the appropriate MCMC sampling method for Bayesian updating. The main feature of the proposed BHM-based SI method is that it utilizes the existing closed-function relationships between structural parameters and responses, as can be seen in the process layer of the BHM structure in Fig. 3. These process characteristics can eliminate the computational effort to configure the CPTs between the structural parameters and the response nodes in the current

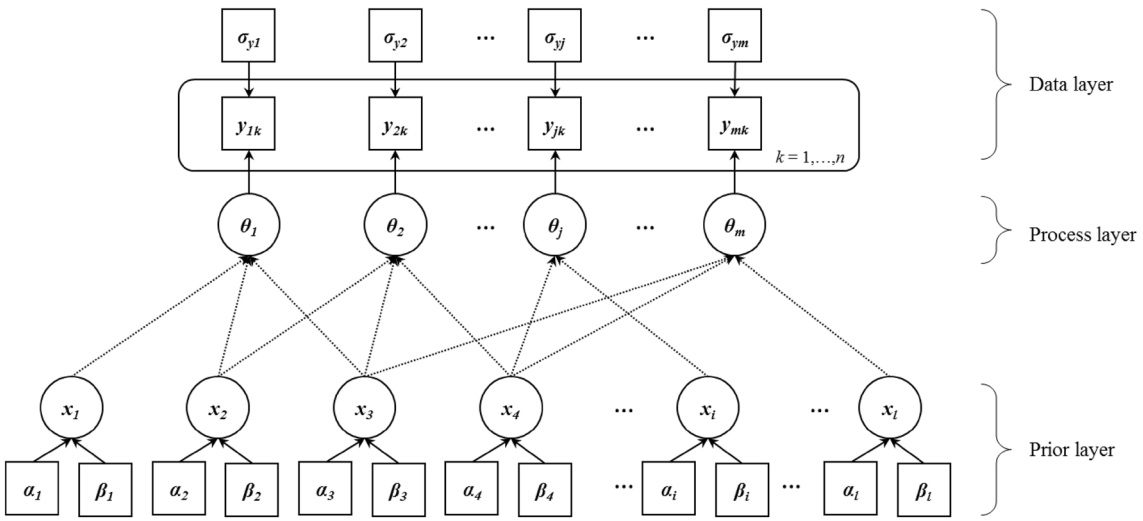

Fig. 3 BHM structure for SI of structural parameters

BN-based SI method setting. In addition, no optimization techniques are required for the proposed method since it adopts the Bayesian updating concept. Accordingly, this avoids the numerical instability issues that can occur in deterministic SI approaches. The effectiveness of the proposed approach will be explained in detail using the application examples in Sect. 4.

4 Example studies: two structural experiments and one realistic slope structure

In this section, the proposed BHM-based approach for the SI of structural system parameters is applied to two experimental structures and one realistic soil-slope structure to explore its effectiveness. The first example demonstrates the applicability of the method to a two-dimensional problem of which the posterior distribution can be graphically represented. The second example demonstrates its applicability to the multi-dimensional problem in which its posterior distribution cannot be recognized visually. The third one demonstrates the applicability of the method to realistic soil-slope structures having an empirical model between seismic loading and output. The results of the proposed approach are verified by comparing the values obtained from the proposed method with the actual measurement results. The field observations are typically limited in the real world. But, from the SI perspective, the acquisition of many data as possible is essential. Thus, the number of observation data were limited to the number of eight in this study. Bayesian updating is implemented using the MCMC sampling method introduced in Sect. 2.1. Specifically, the MH sampling technique is used for the first and the second examples, and the Gibbs sampling scheme is employed in the third example. The total number of samples used in all analyses was 100,000. The language used to implement the proposed method was MATLAB for the first and second examples and R including JAGS [28] for the third example. The detailed pseudo code for each example is presented in the following subsections.

4.1 Two-DOF system under base excitation: two-parameter problem

Prediction of the stiffness of an actual structure can be utilized as a major predictor of damage to the structure. For example, the degree of damage in a structure can be evaluated through the difference between the stiffness values obtained based on the information of the original designed structure and the stiffness estimated through the measurement on the characteristics of the structure. In addition, it is very important to determine the dynamic characteristics of the structure because they are critical for the overall response of the structure to dynamic loads such as earthquakes and winds. For example, if the natural frequency of the structure and the excitation frequency of the dynamic loadings coincide with each other, a resonance phenomenon can occur, and responses of the structure will be amplified even under small loadings. Such a situation could ultimately cause collapse of the structure. Therefore, it is essential to understand the realistic natural frequencies of existing structures. The natural frequency of a structure is mathematically a function of the mass and stiffness of the system and can be measured using various field tests. Given this background, we conducted the following small-scale experiment, the main focus of which was to obtain the fundamental frequencies of small-scale structural systems and to measure their stiffnesses. The reason we performed this test on a small scale was to allow comparison of the SI results of the proposed approach with those of the actual measurements. In the following paragraph, we discuss the performance of this test.

Experimental setup The specimen is a two-degree-of-freedom (DOF) system in which the first two natural frequencies were obtained from the forced vibration test (a shake table test). Its natural frequencies under harmonic base excitation were observed by visual inspection based on the results of a magnification factor and phase-angle plots. The vibration test was conducted by fixing the amplitude (u_{go}) of the harmonic excitation, but changing its excitation frequency ($\Omega = 0.5$ Hz $- 20$ Hz in 0.1 Hz increments). Figure 4 shows a configuration of the shake-table test setup. A shaker generates a sine-wave harmonic motion at a certain frequency. A shake table moves horizontally. The base of the two-DOF shear building is fixed to the shake table. Specifically, the two-DOF building consists of two masses that are girders of the building and supporting columns, as shown in Fig. 5. The two columns supporting each mass represent a single stiffness and indicate the representative resilient resistance to a horizontal action at each floor. The measured masses were $m_1 = m_2 = 0.9894$ kg (2.18125 lb or 0.00565 lb•s^2/in). The masses and columns were made of steel and aluminum, respectively. Accelerometers were attached to the two masses, and the accelerations observed as a type of electrical signal were processed with an oscilloscope. Frequency measurement (f_{1i}° and f_{2i}°) was performed eight times, and the results are summarized in Table 2.

Construction of the BHM Given the two-DOF structural system and the measured data, the BHM was designed, as graphically illustrated in Fig. 6. The following equations are specific mathematical expressions for this constructed BHM:

- Data layer : $f_{1i}^{\circ} \sim N(f_1^b, \sigma_{f1})$; $f_{2i}^{\circ} \sim N(f_2^b, \sigma_{f2})$; $i = 1,\ldots,n$
- Process layer : $f_1^b = f_1(k_1,k_2)$; $f_2^b = f_2(k_1,k_2)$;
- Prior layer : $k_1 \sim N(\mu_{k1}, \sigma_{k1})$; $k_2 \sim N(\mu_{k2}, \sigma_{k2})$;

where k_1 and k_2 are the floor stiffnesses following the prior distribution of the normal distribution with mean (μ_{k1} or μ_{k2}) and standard deviation (σ_{k1} or σ_{k2}), and f_1^b and f_2^b are

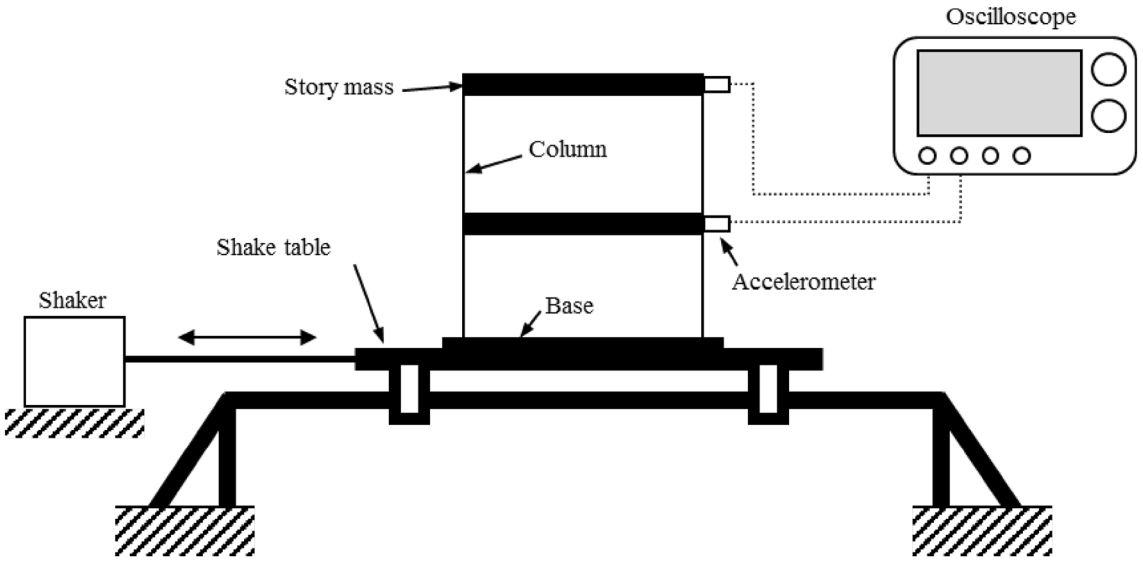

Fig. 4 Configuration of the shake table test setup

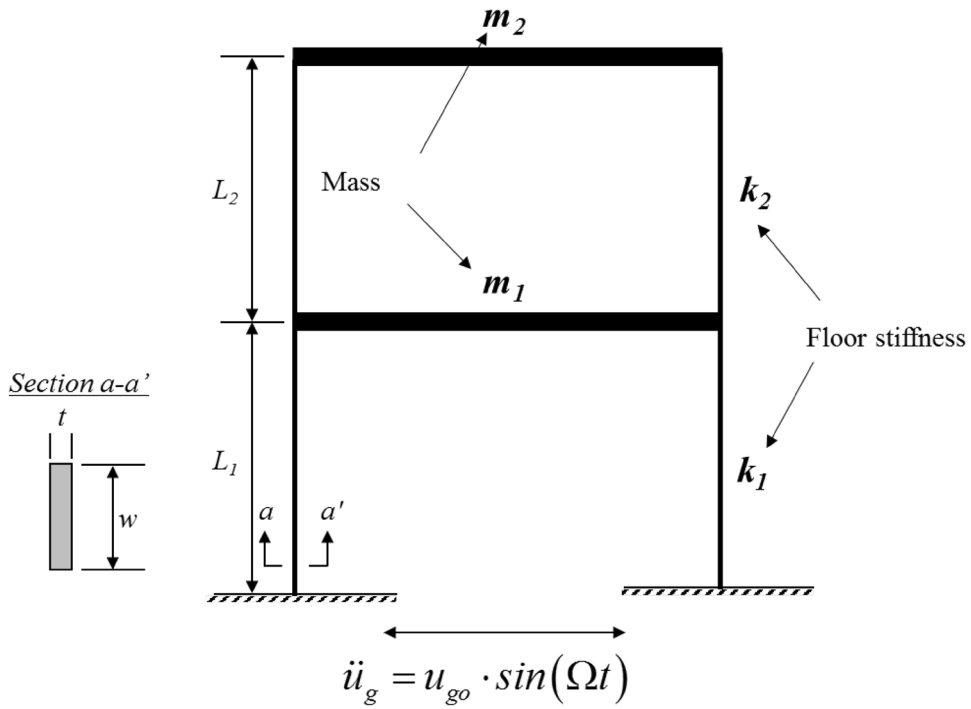

Fig. 5 Mathematical model of the 2-DOF system

Table 2 Frequency observation from the shake table test

	$i=1$	$i=2$	$i=3$	$i=4$	$i=5$	$i=6$	$i=7$	$i=8$
f_{1i}° (Hz)	5.7	5.9	5.8	5.9	6.0	5.9	5.9	6.1
f_{2i}° (Hz)	15.1	15.4	15.0	15.4	15.7	15.3	15.4	15.7

theoretically calculated natural frequencies from Eigen-analysis of the structure in Eq. [5]:

$$|\mathbf{K} - \omega_i \cdot \mathbf{M}| = 0, f_i^b = \omega_i/(2 \cdot \pi); \quad i = 1, 2 \tag{5}$$

where **K** is the stiffness matrix obtained from k_1 and k_2 (i.e., $[k_1+k_2,\text{-}k_2;\text{-}k_2,k_2]$); **M** is the mass matrix consisting of m_1 and m_2 (i.e., $[m_1,0;0,m_2]$); and ω_i is the angular natural

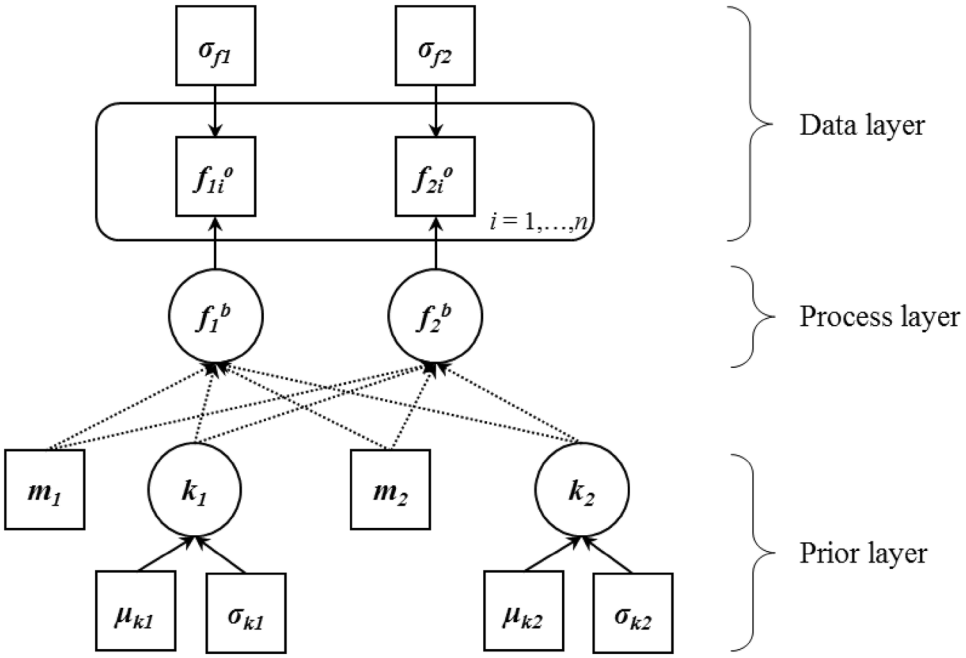

Fig. 6 BHM for SI of natural frequencies of a two-DOF structural system

frequencies. Thus, in the process layer, the function f_1 (−) estimates ${f_1}^b$, and the function f_2 (−) calculates ${f_2}^b$. The measured natural frequencies ${f_{1i}}^\circ$ and ${f_{2i}}^\circ$ of Table 1 are assumed to follow normal distributions having measured error σ_{f1} and σ_{f2}, respectively. Finally, the posterior distribution regarding the prior distribution for the floor stiffnesses k_1 and k_2 can be represented as the following equation:

$$
\begin{aligned}
&p\left(k_1,k_2|\mathbf{f}_1{}^\circ,\mathbf{f}_2{}^\circ\right)\\
&\propto \prod_{i=1}^{n}\left[p\left({f_{1i}}^\circ|{f_1}^b\right)\right]\prod_{i=1}^{n}\left[p\left({f_{2i}^o}|{f_2^b}\right)\right]p\left(f_1^b|k_1,k_2\right)p\left(f_2^b|k_1,k_2\right)p\left(k_1\right)p\left(k_2\right)\\
&=\prod_{i=1}^{n}\left[p\left({f_{1i}}^\circ|f_1\left(k_1,k_2\right)\right)\right]\prod_{i=1}^{n}\left[p\left({f_{2i}}^\circ|f_2\left(k_1,k_2\right)\right)\right]p\left(k_1\right)p\left(k_2\right)
\end{aligned}
\tag{6}
$$

Specifically, the properties for prior distributions of k_1 and k_2 are $\mu_{k1}=\mu_{k2}=2.63$ kN/m (15 lb/in) and $\sigma_{k1}=\sigma_{k2}=0.1\bullet 2.63$ kN/m ($0.1\bullet 15$ lb/in), respectively, and the measurement errors are $\sigma_{f1}=0.3$ Hz and $\sigma_{f2}=0.3$ Hz. The number of data points measured is $n=8$. The MATLAB-type pseudo code for example 1 is given in Table 3.

4.1.1 BHM results

Because example 1 is a two-parameter SI problem, the results can be visually described in two-dimensional space. Figure 7 shows prior and likelihood distributions and the joint posterior distribution using Eq. [6] in k_1–k_2 dimensional

Table 3 Pseudo code for example 1 (MATLAB-type)

```
% Experiment results (from Table 2)
    Y = [5.7;  5.9;  5.8;  5.9;  6.0;  5.9;  5.9;  6.1];
    Z = [15.1; 15.4; 15.0; 15.4; 15.7; 15.3; 15.4; 15.7];
% Prior layer
    muk1 = 2.63; sk1  = 0.1*muk1;
    muk2 = 2.63; sk2  = 0.1*muk2;
% Process & Data layer (from Eq. (5) and Eq. (6))
    Prior1 = @(x) normpdf(x,muk1,sk1);
    Prior2 = @(x) normpdf(x,muk2,sk2);
    fPrior1 = @(x) Fn1(x(1),x(2));  % from Eq.(5)
    fPrior2 = @(x) Fn2(x(1),x(2));  % from Eq.(5)
    like1 = @(x) prod(normpdf(Y,x,0.3));
    like2 = @(x) prod(normpdf(Z,x,0.3));
    Prior = @(x) Prior1(x(1))*Prior2(x(2));
    Like  = @(x) like1(fPrior1(x))*like2(fPrior2(x));
    Post  = @(x) Like(x)*Prior1(x(1))*Prior2(x(2));
% MH sampling (from Table 1)
    MHsampler;
```

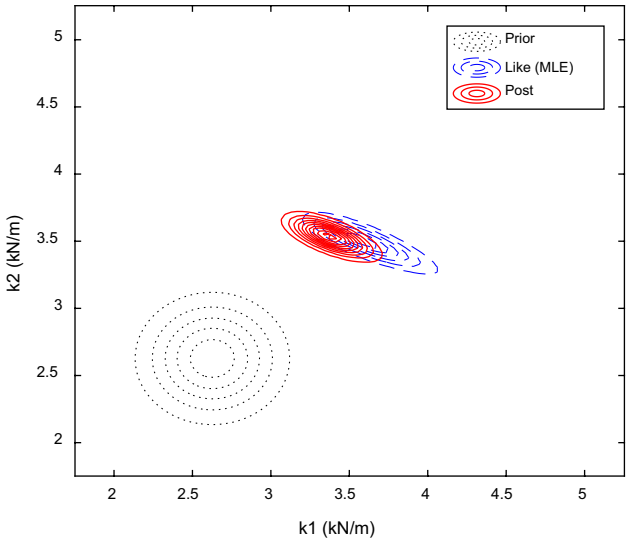

Fig. 7 Prior, likelihood, and posterior distributions for k_1 and k_2

space. As seen from the figure, the prior distribution was updated to the posterior distribution by accommodating the observed frequencies. Thus, the obtained posterior distribution becomes a targeted distribution from which we need to draw the samples to evaluate characteristics of the posterior distribution. Figure 8a and b show the samples drawn from the targeted posterior distribution for k_1 and k_2. Specifically, Fig. 8c illustrates the graphical process of drawing samples from the targeted region using the MH algorithm. We can see that the drawn samples successfully capture the target posterior distribution except for a few samples in the initial stage. From the obtained samples, excluding the initial samples (also called burn-in samples), the distribution characteristics were identified and are plotted in Fig. 9. To verify the result of the proposed method, the actual measurement of the floor stiffnesses k_1 and k_2 is conducted and compared with the results of the proposed approach. Also, these results are compared with those obtained when using the MLE technique of the traditional statistics approach. The floor stiffness can be measured by summing the stiffness of the two columns. Each column's stiffness can be estimated using the measured dimensions of a column (width w, thickness t, and length L). The theoretical stiffness calculation for each column is $12 \bullet E \bullet I/L^3$, where $I = w \bullet t^3/12$. The actual measured floor stiffness is plotted in Fig. 9 along with the result of the proposed method. As shown in this figure, the comparison with the actual measurement results reveals that the proposed method well identifies both system parameters of k_1 and k_2 under the uncertain conditions. From the results above, several important findings can be summarized as follows: (a) no additional computation efforts were necessary to construct the probabilistic relationship between the floor stiffness and natural frequencies compared to the BN-based SI method, as this relationship was already given in Eq. [5]. Hence, this method shows computational efficiency; and (b) compared to the results of the MLE approach using only the likelihood function (see Fig. 9), the proposed approach provided relatively accurate results. Further, the changes in the results of the proposed method were smaller than those of the MLE technique. This indicated that the proposed method could provide more confident results with a narrower distribution compared to MLE. Figure 9 graphically illustrates these results and observations. Table 4 specifically compares the results obtained from the MLE method, proposed approach, and actual measurements. From this table, we quantitatively confirm that the performance of the proposed approach is better than the existing MLE approach. This assertion also coincides with a previous study utilizing the Bayesian updating concept [24]. Consequently, these findings can be similarly applied to the high-dimensional examples in the following subsections. Thus, for brevity, in the following subsections, we will focus on the accuracy of the proposed method in comparison with actual measurements.

4.2 Cantilever beam under a concentrated load: multiple-parameter problem 1

The displacements of the structure can be easily observed under normal static loads, and based on this information, the state of the structure can be assessed. Specifically, the state of the structure can be determined by estimating the stiffness through the observed displacement. The stiffness of a typical static structure depends on the cross-sectional shape of the structure. Thus, the estimation of the dimensions of the cross-section is essential. For example, let us suppose that certain damage to an originally designed structure occurs and a change in cross-section appears in the actual structure. In such a situation, the displacement of the actual structure with respect to the static load will be different from the predicted value of the originally designed structure. In this case, it is not possible to measure the dimensions in real-life or complex structural systems, so a proper method to predict them will be required. Under this circumstance, as an example, this experiment was conducted to obtain the displacement responses of small-scale cantilever beams subject to a concentrated load, as well as to measure their dimensions. Similar to example 1, the main purpose of this scale example was to compare the SI results of the proposed approach with those of actual measurements. In the following paragraph, we discuss how to conduct this experiment.

Experimental setup This example is a cantilever beam subjected to a vertical concentrated load at the free end of the beam. The test is to measure the vertical displacement of the cantilever beam at the free end, which is a vertical loading location, using an LVDT (linear variable differential transformer) test setup. Figure 10 shows a configuration of

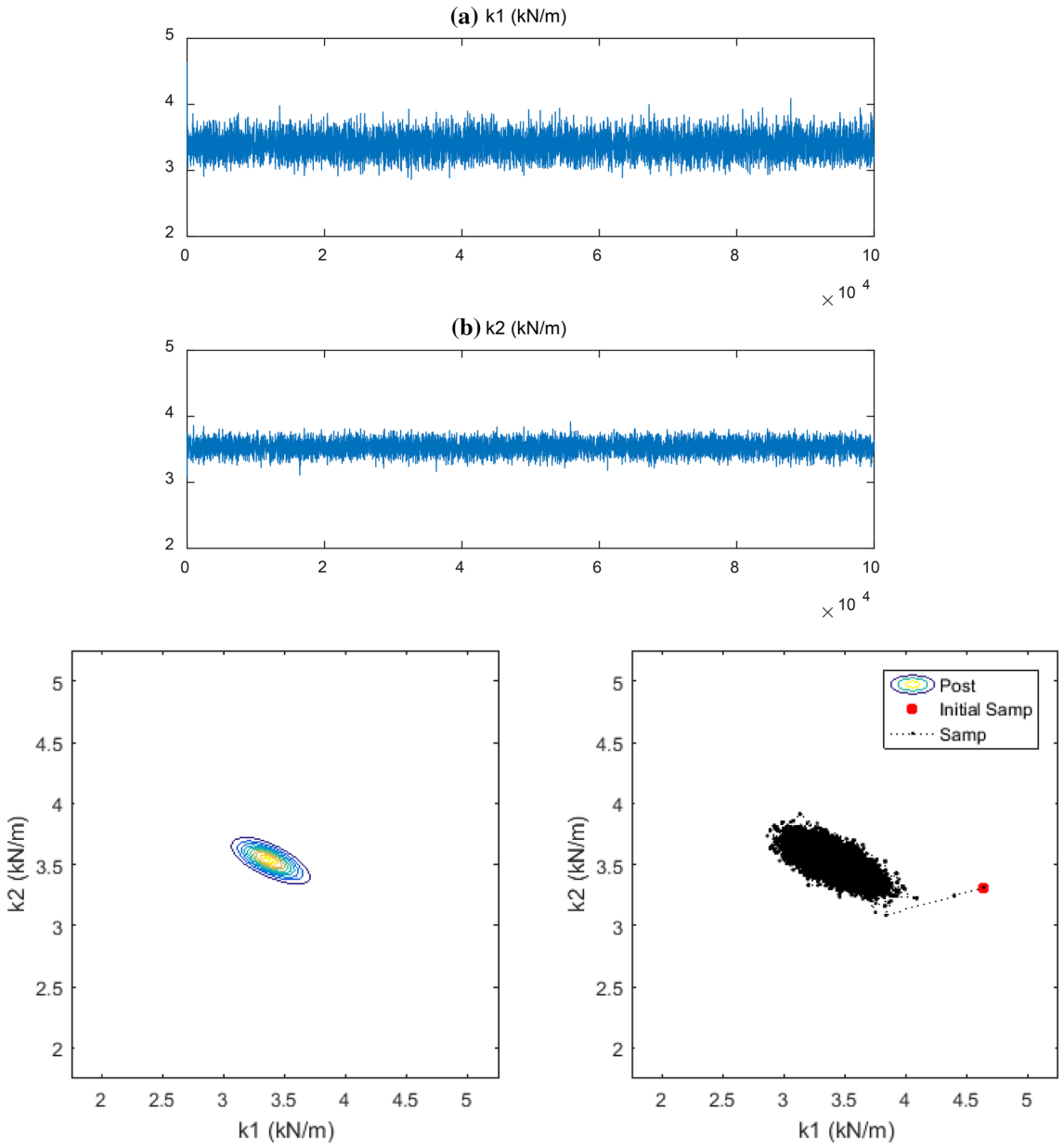

(c) Samples from a k_1-k_2 joint posterior distribution

Fig. 8 MCMC samples from a joint posterior distribution of k_1 and k_2

the LVDT test setup for this purpose. The pin of the LVDT is vertically installed on the surface of the cantilever beam at the free end on which the concentrated load is placed. The LVDT is connected to the power supply to create the electrical signals and wired into a DMM (digital multi-meter) to read the corresponding electrical values. The vertical displacements at the free end ($D_i°$) are measured eight times, and the results are summarized in Table 5. Figure 11 shows the idealized model intended to obtain the vertical displacement of the cantilever beam subjected to a vertical concentrated load at the free end.

Construction of BHM Given the mathematical model for obtaining the displacement of the cantilever beam and the measured data, the BHM can be formulated. Figure 12 shows a graphical illustration of the BHM. The following are the detailed mathematical formulations for this:

- Data layer : $D_i° \sim N(D^b, \sigma_D)$; $i = 1,\ldots,n$
- Process layer : $D^b = f(E, b, h, L)$;
- Prior layer : $E \sim N(\mu_E, \sigma_E)$; $b \sim N(\mu_b, \sigma_b)$; $h \sim N(\mu_h, \sigma_h)$; $L \sim N(\mu_L, \sigma_L)$;

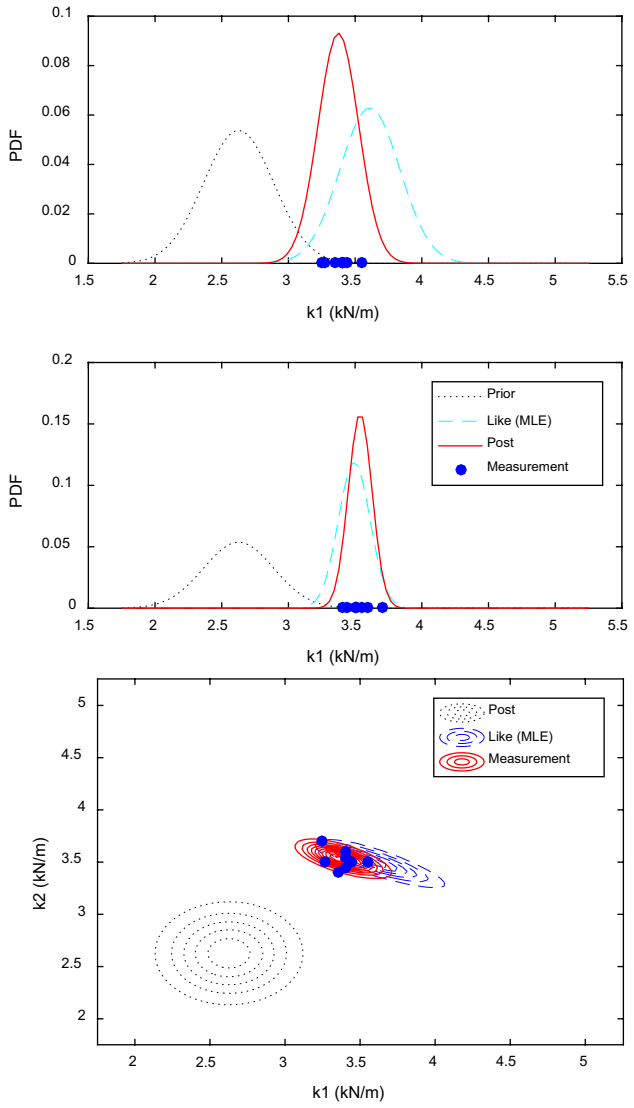

Fig. 9 Prior and posterior distributions and experimental measurements: example 1

where E is Young's modulus; b and h are the dimensions of a square section of cantilever beam; L is the entire length of the cantilever beam from the fixed end to the free end; E, b, h, and L are the prior distributions of the normal distributions with mean values μ_E, μ_b, μ_h, and μ_L and standard deviations σ_E, σ_b, σ_h, and σ_L, respectively. Here, D^b is the theoretically estimated displacement from the Bernoulli–Euler beam theory as $P{\cdot}L^3/(3{\cdot}E{\cdot}I)$, where P is the applied load at the free end, and I is the second moment of inertia for the axis about which the beam is bending. This is $b{\cdot}h^3/12$ for the squared section. The measured displacements D_i° shown in Table 5 are assumed to follow normal distributions with measured error σ_D. Finally, the posterior distribution regarding the prior distribution for stochastic variables E, b, h, and L can be represented as follows:

Table 4 Comparison results of MLE, BHM (proposed method), and actual measurement

Parameters	Mean		
	MLE	BHM (proposed)	Actual measurement
k_1 (N/m)	3.6126	3.3769	3.3825
k_2 (N/m)	3.4913	3.5333	3.5238
Parameters	Standard deviation		
	MLE	BHM (proposed)	Actual measurement
k_1 (N/m)	0.2293	0.1469	0.0953
k_2 (N/m)	0.1198	0.0860	0.0938
Parameters	Mean Error (%)		
	MLE	BHM (proposed)	Actual measurement
k_1 (N/m)	6.80	0.17	-
k_2 (N/m)	0.92	0.27	-

$$
\begin{aligned}
&p\left(E,b,h,L|\mathbf{D^o}\right)\\
&\propto \prod_{i=1}^{n}\left[p\left(D_i^{\circ}|D^b\right)\right]p\left(D^b|E,b,h,L\right)p(E)p(b)p(h)p(L)\\
&=\prod_{i=1}^{n}\left[p\left(D_i^{\circ}|f(E,b,h,L)\right)\right]p(E)p(b)p(h)p(L)
\end{aligned}
\tag{7}
$$

where $f(-)$ is the theoretically calculated displacement for D^b. In this example, the properties for prior distributions of E, b, h, and L are $\mu_E = 75.88$ GPa (1.1e7 psi), $\mu_b = 27.94$ mm (1.1 in), $\mu_h = 12.7$ mm (0.5 in), $\mu_L = 203.2$ mm (8 in), and $\sigma_E = 7.59$ GPa (0.1·1.1e7 psi), $\sigma_b = 2.79$ GPa (0.1·1.1 in), $\sigma_h = 1.27$ mm (0.1·0.5 in), $\sigma_L = 20.32$ mm (0.1·8 in). P is set to 66.72 N (15 lb), and the measurement error is $\sigma_D = 0.23$ mm. The number of data points measured is $n = 8$. The MATLAB-type pseudo code for implementing example 2 is given in Table 6.

4.2.1 BHM results

The targeted posterior distribution is obtained using Eq. (7). Figure 13 shows the samples drawn based on this targeted joint posterior distribution for E, b, h, and L. Because example 2 is a four-parameter SI problem, the joint posterior distribution cannot be visually identified. Thus, using the drawn samples without burn-in samples, the characteristics of the marginal distributions of the parameters are derived and plotted in Fig. 14. For the purpose of comparison, the measured E, b, h, and L are plotted along with the results of the proposed method. As shown in these figures, the comparison with the measurement results illustrates that the proposed

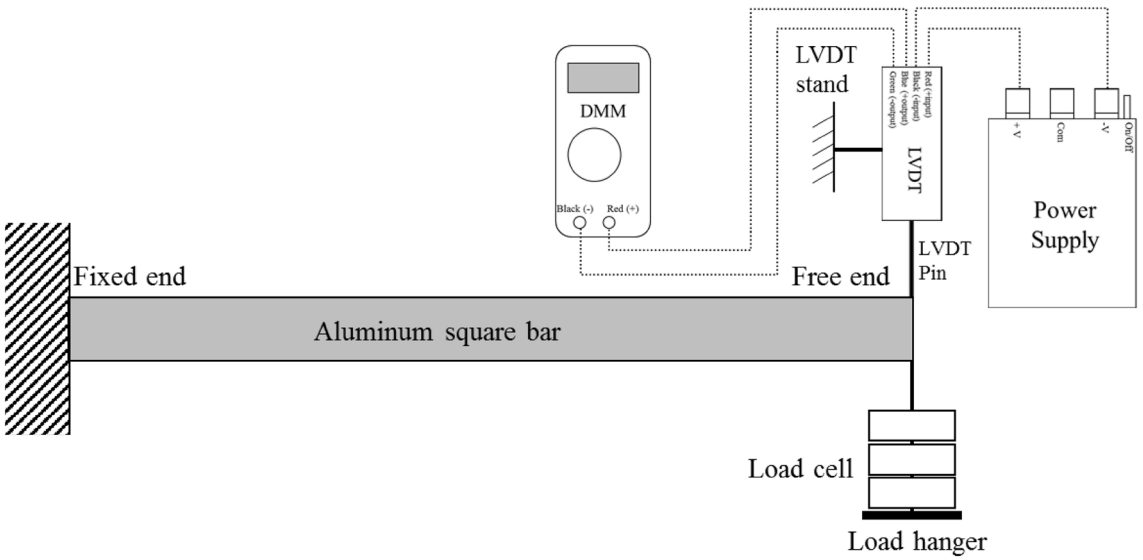

Fig. 10 Configuration of the LVDT test setup for measuring free-end displacement of a cantilever beam

Table 5 Measured displacement from the LVDT test (test result)

	$i=1$	$i=2$	$i=3$	$i=4$	$i=5$	$i=6$	$i=7$	$i=8$
D_i° (mm)	4.70	4.89	4.25	4.58	4.63	4.00	4.19	4.37

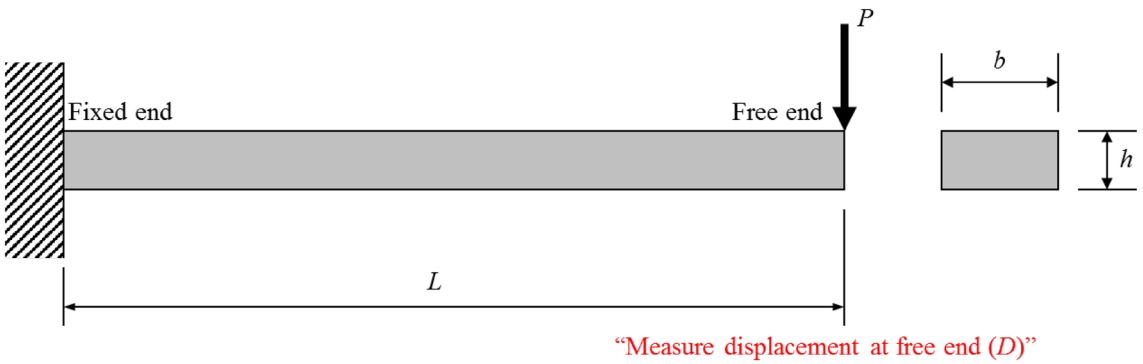

Fig. 11 Mathematical model for obtaining vertical displacement of a cantilever beam subjected to a vertical concentrated load at the free end

method well captures the four-system parameters of *E, b, h*, and *L*, as in Example 1.

4.3 Soil-slope structure under earthquakes: multiple-parameter problem 2

Empirical permanent displacement of a slope structure subjected to earthquake ground motion The methods developed to evaluate the stability and performance of slopes during earthquakes are divided into three groups: (1) pseudo-static analysis, (2) stress deformation analysis, and (3) permanent displacement analysis (also called the Newmark method). Of the three, the Newmark method is widely known as a compromise between the crude assumption of pseudo-static analysis and the difficulties of stress deformation analysis. Laboratory tests [29] and earthquake-induced landslide analyses on a natural slope [30] verified that the Newmark method fairly accurately predicts slope displacements if the slope geometry, soil properties, and earthquake ground motions are known. The method treats a landslide as a rigid-plastic body: the mass does not deform internally, there is no permanent displacement at accelerations below the critical level, and the mass deforms plastically along a discrete basal

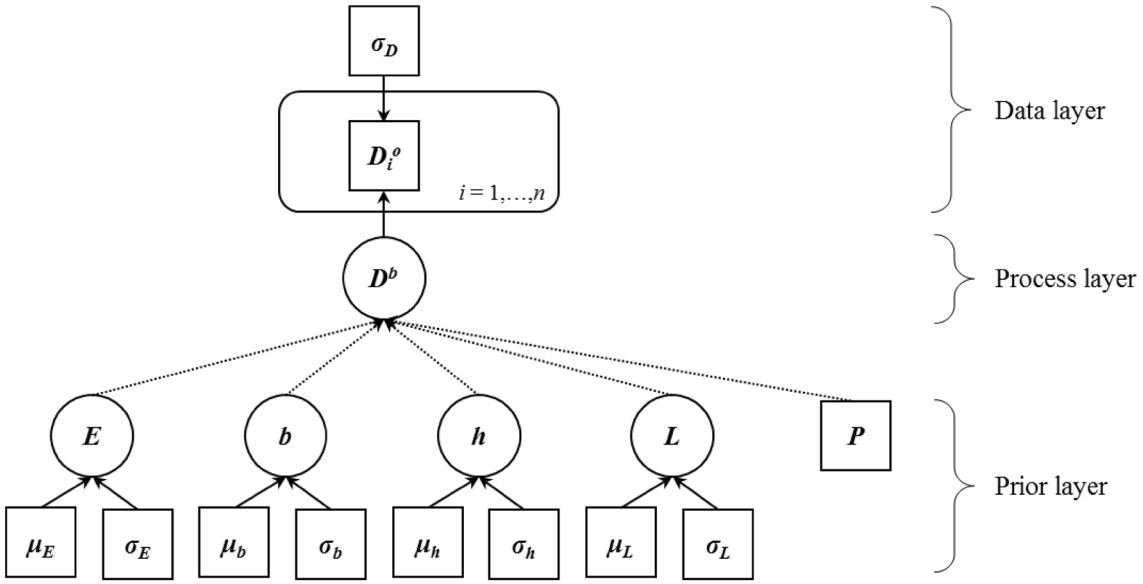

Fig. 12 BHM for SI of displacement of the cantilever beam subjected to a point load at the free end

Table 6 Pseudo code for example 2 (MATLAB type)

```
% Experiment results (from Table 5)
    Y = [4.70; 4.89; 4.25; 4.58; 4.63; 4.00; 4.19; 4.37];
% Prior layer
    muE = 1.1; sE  = 0.1*muE;
    mub = 1.1; sb  = 0.1*mub;
    muh = 0.5; sh  = 0.1*muh;
    muL = 0.8; sL  = 0.1*muL;
% Process & Data layer (from Eq.(7))
    Prior1 = @(x) normpdf(x,muE,sE);
    Prior2 = @(x) normpdf(x,mub,sb);
    Prior3 = @(x) normpdf(x,muh,sh);
    Prior4 = @(x) normpdf(x,muL,sL);
    fPrior = @(x) DEL(x(1),x(2),x(3),x(4));  % from Bernoulli-Euler beam theory (PL3/(3EI)
    like   = @(x) prod(normpdf(Y,x,0.23));
    Like   = @(x) like(fPrior(x));
    Post   = @(x) Like(x)*Prior1(x(1))*Prior2(x(2))*Prior2(x(3))*Prior2(x(4));
% MH sampling (from Table 1)
    MHsampler;
```

shear surface when the critical acceleration is exceeded. Since the method was introduced by Newmark [31], it has been improved [32]. Moreover, based on the concept and past earthquake ground-motion record histories, various empirical models have been proposed [33]. This paper employs the model proposed by Ambraseys and Menu [34], developed after Newmark analyses of 50 strong ground-motion records from 11 earthquakes. For the SI study of this research, as an experimental result, permanent displacements of slope were artificially generated from the situation where a particular slope with specific parameters was subjected to 1·g peak ground acceleration (PGA)-intensity-level ground-motion. The artificially generated displacements D_{ni}° of Table 7 are assumed to follow normal distributions with measured error σ_{Dn}. The results are illustrated in Table 7. Figure 15 shows an idealized model intended to obtain permanent displacement of a slope subjected to earthquake ground motion.

Construction of BHM Given the empirical model for obtaining the permanent displacement of slope and the measured data, the BHM can be formulated, as shown in Fig. 16. The following formulations shows the detailed mathematical expressions for this:

- Data layer : $D_{ni}^{\circ} \sim N(D_n^b, \sigma_{Dn})$; $i = 1,\ldots,n$
- Process layer : $D_n^b = f_3\ (a_c,\ a_{max})$; $a_c = f_2\ (FS,\ \alpha)$; $FS = f_1\ (c,\ \varphi,\ \alpha,\ \gamma,\ t)$

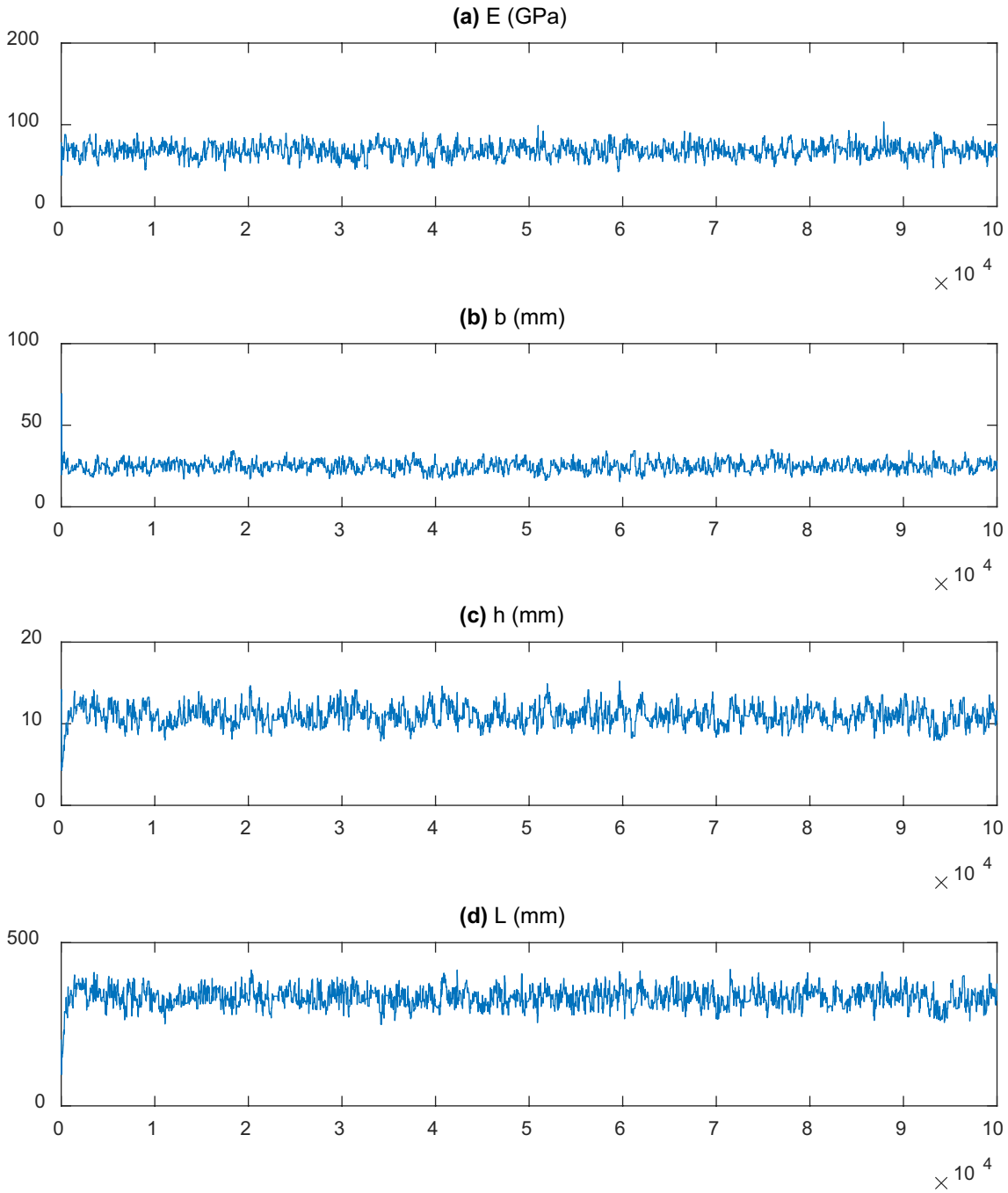

Fig. 13 MCMC samples from joint posterior distributions of *E, b, h*, and *L*

- Prior layer : $c \sim U\,(c_l, c_u)$; $\varphi \sim U\,(\varphi_l, \varphi_u)$; $\alpha \sim U\,(\alpha_l, \alpha_u)$; $\gamma \sim U\,(\gamma_l, \gamma_u)$; $t \sim U\,(t_l, t_u)$

  where c is the effective cohesion; φ is the effective friction angle; α is the slope angle; γ is the unit weight of soil; t is the slope normal thickness of the failure surface; c, φ, α, γ, and t are the prior distributions of the uniform distributions with a certain range; $a_{\max}$ is the PGA (in units of acceleration of gravity g); and ${D_n}^b$, a_c, and FS are the permanent displacement (unit: cm), critical acceleration (unit: g), and the factor of safety, respectively. They are theoretical or empirical values estimated using the following equations [34]:

$$\log\left({D_n}^b\right) = 0.90 + \log\left[\left(1 - \frac{a_c}{a_{\max}}\right)^{2.53}\left(\frac{a_c}{a_{\max}}\right)^{-1.09}\right] \quad (8)$$

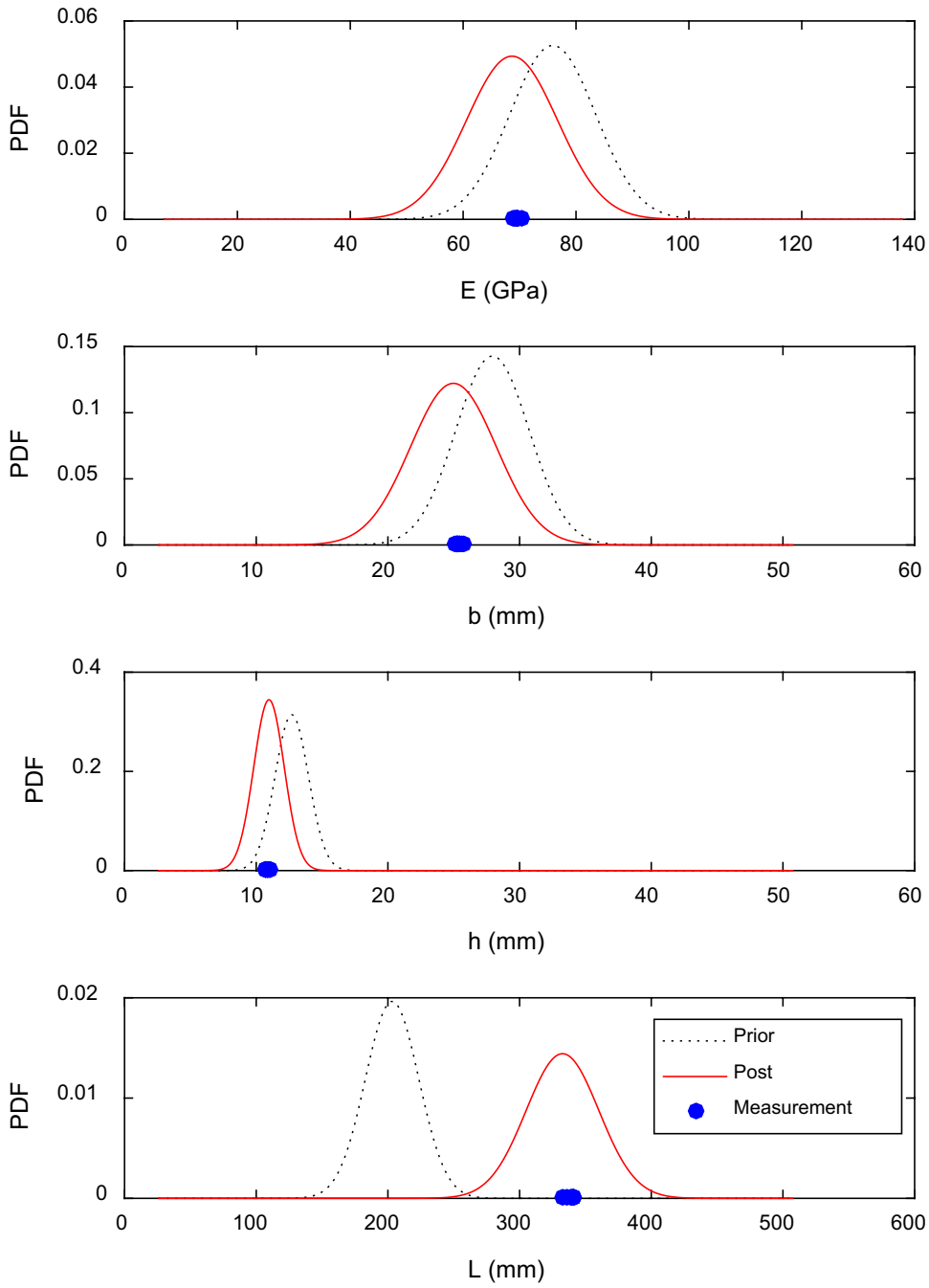

Fig. 14 Prior and posterior distributions and experimental measurement: example 2

Table 7 Artificially generated permanent displacements for a slope subjected to earthquake ground motion with a particular intensity

	$i=1$	$i=2$	$i=3$	$i=4$	$i=5$	$i=6$	$i=7$	$i=8$	$i=9$
D_{ni}°(cm)	5.33	6.21	5.63	4.79	4.94	4.41	4.93	5.76	5.38

$$a_c = (FS - 1) \cdot \sin(\alpha) \tag{9}$$

$$FS = \frac{c}{\gamma \cdot t \cdot \sin(\alpha)} + \frac{\tan(\varphi)}{\tan(\alpha)} - \frac{\gamma_w \cdot m \cdot \tan(\varphi)}{\gamma \cdot \tan(\alpha)} \tag{10}$$

where m is the saturation percentage of failure thickness, and γ_w is the unit weight of water. In this study, m and γ_w are regarded as deterministic variables, and it is assumed that no pore-water pressure is included ($m=0$). Here, the standard deviation of the model in Eq. (8) was ignored

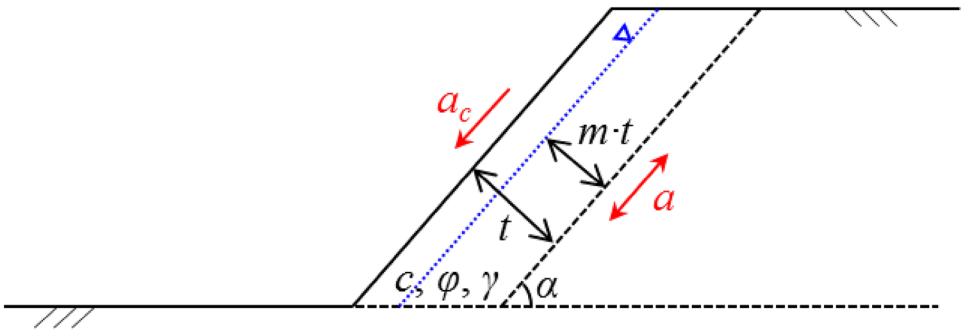

Fig. 15 Sliding block model used for Newmark analysis

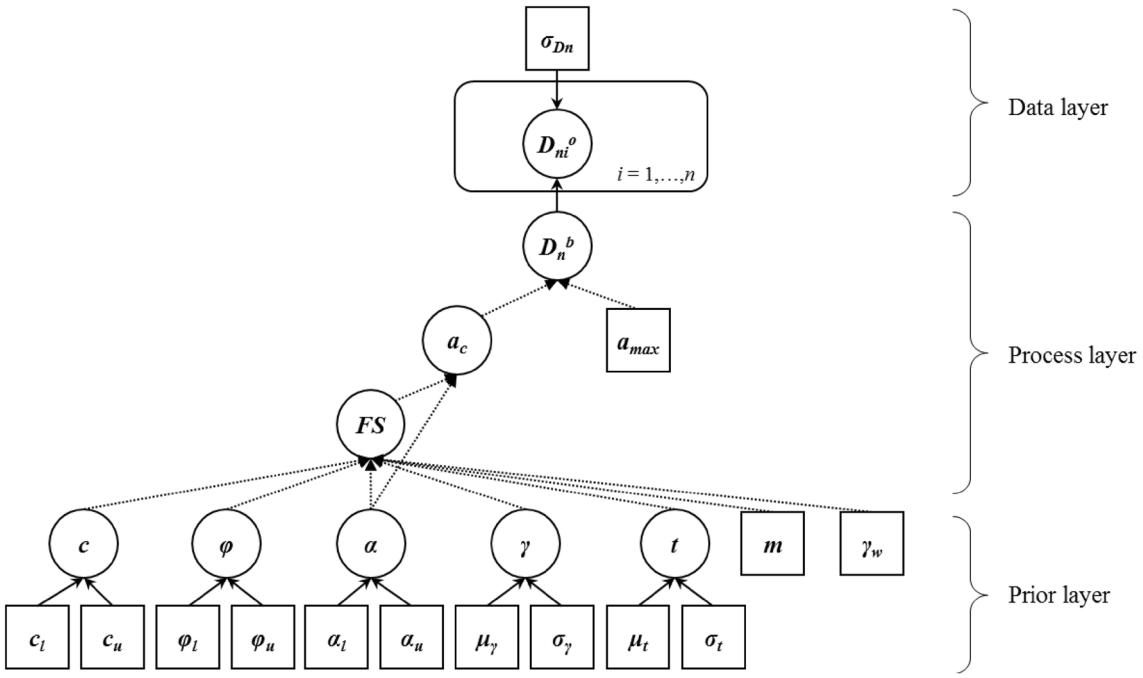

Fig. 16 BHM for SI of Newmark permanent displacement

since this study focused on the median/mean behaviors of the slope when implementing the SI for the structural parameters. Finally, the posterior distribution regarding the prior distribution for stochastic variables c, φ, α, γ, and t can be represented as follows:

$$\begin{aligned} & p\left(c,\varphi,\alpha,\gamma,t|\mathbf{D_n^o}\right) \\ & \propto \prod_{i=1}^{n}\left[p\left(D_{ni}^{o}|D_n^b\right)\right]p\left(D_n^b|c,\varphi,\alpha,\gamma,t\right)p(c)p(\varphi)p(\alpha)p(\gamma)p(t) \\ & = \prod_{i=1}^{n}\left[p\left(D_{ni}^{o}|f(c,\varphi,\alpha,\gamma,t)\right)\right]p(c)p(\varphi)p(\alpha)p(\gamma)p(t) \end{aligned} \tag{11}$$

where $f(-)$ calculates the displacement for D_n^b using Eq. (8)–Eq. [10]. In this example, the properties for prior distributions of c, φ, α, γ, and t are $c_l = 16{,}000$ Pa, $c_u = 26{,}000$ Pa, $\varphi_l = 30°$, $\varphi_u = 40°$, $\alpha_l = 10°$, $\alpha_u = 70°$, $\gamma_l = 14{,}000$ N/m^3, $\gamma_u = 17{,}000$ N/m3, $t_l = 2.2$ m, and $t_u = 2.6$ m. The measurement error is $\sigma_{Dn} = 0.25$ cm, and the number of data points measured is $n = 9$. The pseudo code for example 3 in the type of R and JAGS is given in Table 8.

4.3.1 BHM results

The targeted posterior distribution was obtained using Eq. [11], and the samples were drawn from this targeted distribution. Similar to the previous examples, the distribution characteristics were estimated based on the obtained samples (excluding the burn-in samples), and the results are illustrated in Fig. 17. For the purpose of comparison, the values of the variables of c, φ, α, γ, and t that are used to artificially generate the simulated observations of Table 7 are plotted

Table 8 Pseudo code for example 3 (R JAGS type)

```
# Experiment results (from Table 7)
    Y  <- c(5.33, 6.21, 5.63, 4.79, 4.94, 4.41, 4.93, 5.76, 5.38)
# Bayesian updating by R JAGS
    library(rjags)
    model_string <- "model{
    # Data layer: Likelihood
    for(i in 1:nY){
    Y[i]  ~ dnorm(DN,(0.05*5)^2)
    }
# Process layer (from Eq.(8), Eq.(9) and Eq.(10)
    Calculate FS
    Calculate ac
    Calculate DN
# Prior layer
    c   ~ dunif(16000,26000)
    phi ~ dunif(30,40)
    alp ~ dunif(10,70)
    r   ~ dunif(14000,17000)
    t   ~ dunif(2.2,2.6)
    }"
# Gibbs sampling
    Gibbssampler;
```

along with the results of the proposed method. Specifically, such values were extracted given normal distributions with mean values of $c = 21{,}000$ Pa, $\varphi = 35°$, $\alpha = 42°$, $\gamma = 15{,}500$ N/m^3, $t = 2.4$ m and coefficients of variations = 0.01. As shown in these illustrations, the comparison with the artificial measurement results shows that the proposed method well selects all system parameters of c, φ, α, γ, and t, as in the results of previous examples.

5 Summary and conclusions

This study focused on the development of a novel approach for the system identification (SI) of structural system parameters. The reason for this development was that the current deterministic SI approach had some issues such as non-stability and non-uniqueness of solutions, and that the probabilistic SI method based on a Bayesian network bore a large computational cost to construct conditional probability tables (CPTs) between structural parameter and response output nodes. Therefore, to overcome these limitations, the concepts of a Bayesian hierarchical model (BHM) technique were combined with a Bayesian updating framework instead of utilizing the discrete Bayesian network scheme. In Bayesian statistics, the BHM is a common concept in estimating the parameters of posterior distributions. The correctness of the BHM has already been proved, theoretically [25]. The merit of such technique is prominent when data/information are available on several different levels of observational units. The proposed BHM-based SI approach enabled utilization of the existing relations between structural parameters and responses, which was given in closed function form. This could eliminate the computational efforts needed to construct CPTs between parameter and response nodes. Also, the proposed approach embedded in the Bayesian updating did not need any optimization, so the ill-posedness problems that might occur in the deterministic SI approach could be avoided.

The effectiveness of the proposed BHM-based SI method was successfully verified by application to two experimental structures and a realistic soil-slope structure. Comparison of the calculated and actual measurement results showed that the proposed method well identified uncertain structural system parameters. In addition, the proposed SI approach provided relatively accurate and confident estimation results compared to the maximum likelihood estimation approach. Thus, the proposed approach can be utilized to address SI problems for complex structural systems and their computational models by integration with a statistical regression approach or various machine learning algorithms, which will be considered in future studies.

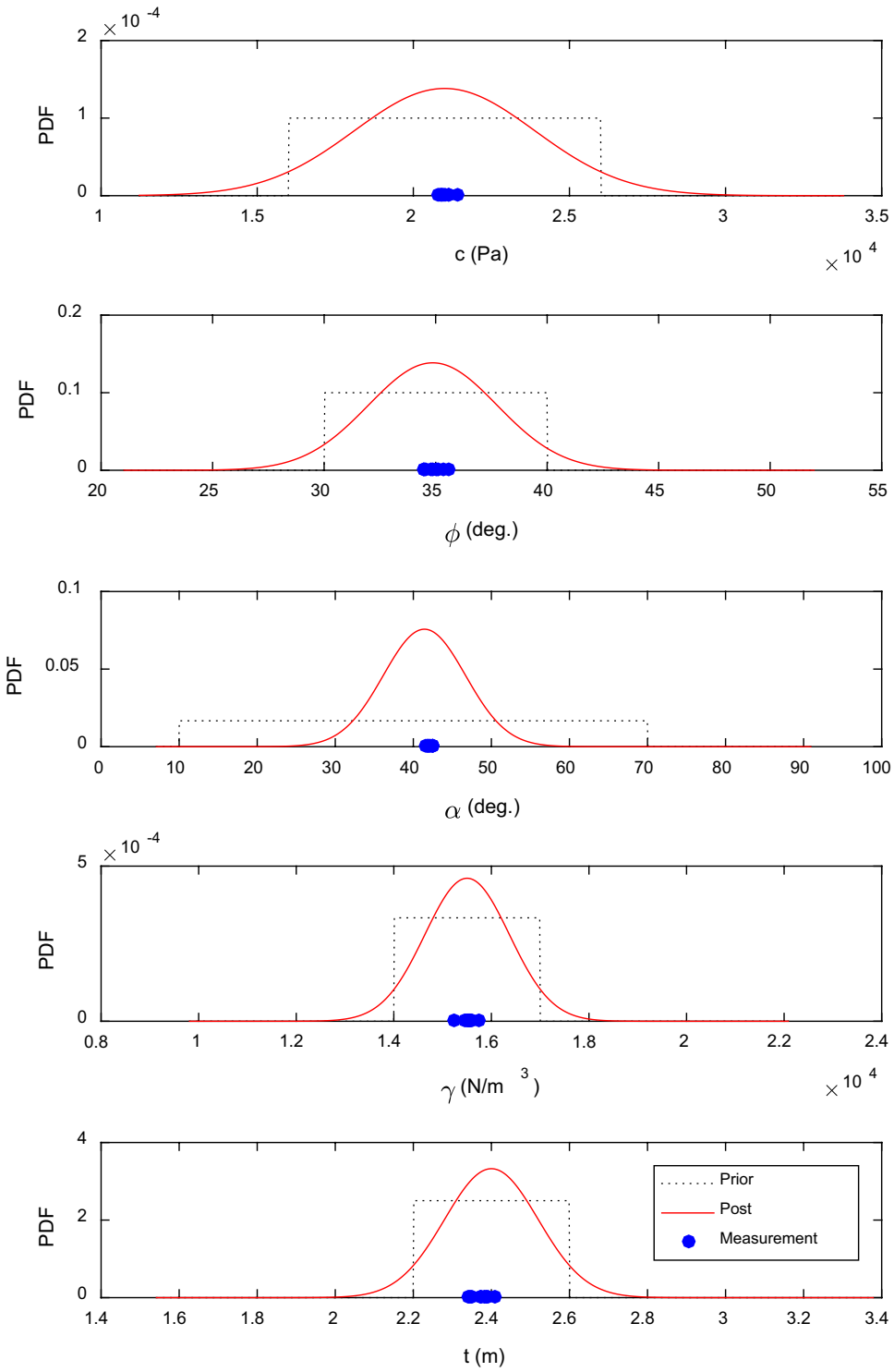

Fig. 17 Prior and posterior distributions and measurement: example 3

Acknowledgements This work was supported by a National Research Foundation of Korea (NRF) grant funded by the Korean government (Ministry of Science, and ICT) (NRF-2017M2A8A4015290 and NRF-2017R1C1B1002855). These supports are gratefully acknowledged.

References

1. Farrar CR, Worden K (2012) Structural health monitoring: a machine learning perspective. Wiley, New York
2. Annamdas VGM, Bhalla S, Soh CK (2017) Applications of structural health monitoring technology in Asia. Struct Health Monit 16(3):324–346

3. Nelles O (2013) Nonlinear system identification: from classical approaches to neural networks and fuzzy models. Springer, Berlin
4. Ladeveze P, Rougeot P (1997) New advances on a posteriori error on constitutive relation in FE analysis. Comput Methods Appl Mech Eng 150(1–4):239–249
5. Louf F, Charbonnel PE, Ladeveze P, Gratien C (2008) An updating method for structural dynamics models with unknown excitations. J Phys Conf Ser 135(1):12065 **(IOP Publishing)**
6. Weaver J (2015) The self-optimizing inverse methodology for material parameter identification and distributed damage detection. Ph.D. dissertation, The University of Akron, US
7. Thoft-Christensen P, Murotsu Y (2012) Application of structural systems reliability theory. Springer, Berlin
8. Benjamin JR, Cornell CA (1970) Probability. Statistics, and decision for civil engineers. McGraw-Hill, New York
9. Ang AHS, Tang WH (1984) Probability concepts in engineering planning and design. Wiley, New York
10. Beck JL, Katafygiotis LS (1998) Updating models and their uncertainties. I: Bayesian statistical framework. J Eng Mech 124(4):455–461
11. Au SK, Beck JL (2001) Estimation of small failure probabilities in high dimensions by subset simulation. Probab Eng Mech 16(4):263–277
12. Straub D, Papaioannou I (2014) Bayesian updating with structural reliability methods. J Eng Mech 141(3):04014134
13. Beven K (2010) Environmental modelling: an uncertain future?. CRC Press, Boca Raton
14. Weber P, Medina-Oliva G, Simon C, Iung B (2012) Overview on Bayesian networks applications for dependability, risk analysis and maintenance areas. Eng Appl Artif Intell 25(4):671–682
15. Bensi M, Kiureghian AD, Straub D (2014) Framework for post-earthquake risk assessment and decision making for infrastructure systems. ASCE-ASME J Risk Uncertain Eng Syst Part A: Civil Eng 1(1):04014003
16. Kwag S, Gupta A (2016) Bayesian network technique in probabilistic risk assessment for multiple hazards. In: Proceedings of 24th International Conference on Nuclear Engineering (ICONE 24), 26–30 June 2016, Charlotte, NC, US
17. Kwag S, Gupta A (2017) Probabilistic risk assessment framework for structural systems under multiple hazards using Bayesian statistics. Nucl Eng Des 315:20–34
18. Kwag S, Oh J, Lee JM, Ryu JS (2017) Bayesian-based seismic margin assessment approach: application to research reactor system. Earthq Struct. 12(6):653–663
19. Kwag S, Gupta A, Dinh N (2018) Probabilistic risk assessment based model validation method using Bayesian network. Reliab Eng Syst Saf 169:380–393
20. Kwag S, Oh J, Lee JM (2018) Application of Bayesian statistics to seismic probabilistic safety assessment for research reactor. Nucl Eng Des 328:166–181
21. Kwag S, Oh J (2019) Development of network-based probabilistic safety assessment: a tool for risk analyst for nuclear facilities. Prog Nucl Energy 110:178–190
22. Richard B, Adelaide L, Cremona C, Orcesi A (2012) A methodology for robust updating of nonlinear structural models. Eng Struct 41:356–372
23. Ma Y, Wang L, Zhang J, Xiang Y, Liu Y (2014) Bridge remaining strength prediction integrated with Bayesian network and In situ load testing. J Bridg Eng 19(10):04014037
24. Lee SH, Song J (2016) Bayesian-network-based system identification of spatial distribution of structural parameters. Eng Struct 127:260–277
25. Gelman A, Carlin JB, Stern HS, Rubin DB (2014) Bayesian data analysis (vol 2). Chapman and Hall/CRC, Boca Raton
26. Bolstad WM, Curran JM (2016) Introduction to Bayesian statistics. Wiley, New York
27. Kruschke J (2014) Doing Bayesian data analysis: a tutorial with R, JAGS, and Stan. Academic Press, New York
28. Plummer M (2013) rjags: Bayesian graphical models using MCMC. R package version, 3
29. Wartman J, Seed RB, Bray JD (2005) Shaking table modeling of seismically induced deformations in slopes. J Geotech Geoenviron Eng 131(5):610–622
30. Wilson RC, Keefer DK (1983) Dynamic analysis of a slope failure from the 6 August 1979 Coyote Lake, California, earthquake. Bull Seismol Soc Am 73(3):863–877
31. Newmark NM (1965) Effects of earthquakes on dams and embankments. Geotechnique 15(2):139–160
32. Jibson RW (2011) Methods for assessing the stability of slopes during earthquakes—a retrospective. Eng Geol 122(1):43–50
33. Jibson RW (2007) Regression models for estimating coseismic landslide displacement. Eng Geol 91(2):209–218
34. Ambraseys NN, Menu JM (1988) Earthquake-induced ground displacements. Earthq Eng Struct Dyn 16(7):985–1006